Molecular Microbiology (2014) 93(4), 645–663 ■
doi:10.1111/mmi.12677
First published online 14 July 2014

Trypanosoma brucei histone H1 inhibits RNA polymerase I transcription and is important for parasite fitness *in vivo*

Ana C. Pena,[1] Mafalda R. Pimentel,[1] Helena Manso,[1] Rita Vaz-Drago,[1] Daniel Pinto-Neves,[1] Francisco Aresta-Branco,[1] Filipa Rijo-Ferreira,[1] Fabien Guegan,[1] Luis Pedro Coelho,[1†] Maria Carmo-Fonseca,[1] Nuno L. Barbosa-Morais[1,2] and Luisa M. Figueiredo[1*]

[1]*Instituto de Medicina Molecular, Faculdade de Medicina, Universidade de Lisboa, Av. Prof. Egas Moniz, Edifício Egas Moniz, 1649-028 Lisboa, Portugal.*
[2]*Nuffield Department of Obstetrics and Gynaecology, John Radcliffe Hospital, University of Oxford, Oxford OX3 9DU, UK.*

Summary

***Trypanosoma brucei* is a unicellular parasite that causes sleeping sickness in humans. Most of its transcription is constitutive and driven by RNA polymerase II. RNA polymerase I (Pol I) transcribes not only ribosomal RNA genes, but also protein-encoding genes, including variant surface glycoproteins (*VSGs*) and procyclins. In *T. brucei*, histone H1 (H1) is required for *VSG* silencing and chromatin condensation. However, whether H1 has a genome-wide role in transcription is unknown. Here, using RNA sequencing we show that H1 depletion changes the expression of a specific cohort of genes. Interestingly, the predominant effect is partial loss of silencing of Pol I loci, such as *VSG* and procyclin genes. Labelling of nascent transcripts with 4-thiouridine showed that H1 depletion does not alter the level of labelled Pol II transcripts. In contrast, the levels of 4sU-labelled Pol I transcripts were increased by two- to sixfold, suggesting that H1 preferentially blocks transcription at Pol I loci. Finally, we observed that parasites depleted of H1 grow almost normally in culture but they have a reduced fitness in mice, suggesting that H1 is important for host–pathogen interactions.**

Accepted 15 June, 2014. *For correspondence. E-mail lmf@fm.ul.pt; Tel. (+351) 217 999 512; Fax (+351) 217 999 504. †Present address: European Molecular Biology Laboratory, Meyerhofstraße 1, 69117 Heidelberg, Germany.

Introduction

Trypanosoma brucei is a protozoan parasite responsible for sleeping sickness in humans (African Trypanosomiasis). Gene expression in *T. brucei* has several peculiarities, namely genes being transcribed polycistronically and in a constitutive manner. As a result, most of the genome is believed to be continuously transcribed and gene regulation to happen mainly post-transcriptionally (Clayton and Shapira, 2007). Another unusual feature of transcription in trypanosomes is that RNA Polymerase I (Pol I) is not solely dedicated to the transcription of ribosomal RNA (rRNA) genes, but also transcribes loci that encode for abundant surface proteins, such as variant surface glycoprotein (VSGs) and procyclins. Interestingly, so far, Pol I is the only RNA polymerase in *T. brucei* for which regulation at the transcription level was demonstrated (Rudenko *et al.*, 1989; Gunzl *et al.*, 2003).

VSGs are expressed when parasites reside in the bloodstream of the mammalian host. They are required for the parasite to escape the mammalian immune system by a mechanism known as antigenic variation. *VSGs* are expressed from a specialized sub-telomeric locus called a bloodstream expression site (BES), which also harbours other expression-site-associated genes (*ESAGs*). In the genome there are ~ 15 BESs (Hertz-Fowler *et al.*, 2008), only one of which is transcriptionally active at a time. Outside BESs, *T. brucei* also encodes a silent archive of up to around 2000 *VSG* genes and pseudogenes (Marcello and Barry, 2007). Procyclins are a much smaller gene family, composed of three *EP* genes and one *GPEET* gene (reviewed in Pays *et al.*, 2004). They are located in non-telomeric polycistronic units, which also contain procyclin-associated genes (*PAGs*). In bloodstream forms (BSFs), procyclins are kept silent by transcriptional and post-transcriptional mechanisms. These genes are activated in a coordinated manner when parasites differentiate in the gut of the tsetse transmitting fly (reviewed in Navarro *et al.*, 2007).

Chromatin plays an essential role in allowing or restricting the access to DNA of the machineries involved in gene transcription, replication and DNA repair. Nucleosomes are the basic units of chromatin and consist of ~ 145–147 bp of DNA wrapped around an octamer core of histones

that consists of two copies of each of the histones H2A, H2B, H3 and H4 (Sanicola *et al*., 1990; Luger *et al*., 1997). An additional histone, histone H1 (H1) or linker histone, binds to the DNA that links nucleosomes, as well as DNA entering and exiting the nucleosome core (Noll and Kornberg, 1977; Allan *et al*., 1980). The binding of H1 stabilizes nucleosomes and promotes the folding of chromatin (Robinson and Rhodes, 2006). Histone H1 is the least conserved of all histones (Izzo *et al*., 2008). In mouse and humans, histone H1 is encoded by multiple non-allelic genes, which form several protein variants (11 variants in humans) that can differ in their temporal and cell-type expression profiles, chromatin-binding affinities, sub-nuclear localization and post-transcriptional modifications (Izzo *et al*., 2008). In contrast, *Saccharomyces cerevisiae*, *Drosophila melanogaster* and *Tetrahymena thermophila* each have a single H1 gene (Kasinsky *et al*., 2001). In *T. brucei*, a highly divergent unicellular eukaryote (Simpson and Roger, 2004; Dacks *et al*., 2008), histone H1 is encoded by a multigene family.

In vitro studies have extensively shown the properties of H1 in chromatin condensation and transcriptional repression (Thoma *et al*., 1979; Shimamura *et al*., 1989; Laybourn and Kadonaga, 1991; Bednar *et al*., 1998). *In vivo* studies have confirmed that H1 is a global regulator of chromatin architecture (Fan *et al*., 2005; Masina *et al*., 2007; Hashimoto *et al*., 2010). However, these studies also revealed that H1 is not a global transcription repressor, but rather regulates the transcription of specific sets of genes by a yet unknown mechanism (Shen and Gorovsky, 1996; Hellauer *et al*., 2001; Fan *et al*., 2005). H1 is also involved in other biological processes, including inhibition of DNA repair, telomere maintenance in yeast and mammalian cells (Downs *et al*., 2003; Murga *et al*., 2007), silencing of retrotransposons at the rDNA locus in *D. melanogaster* (Vujatovic *et al*., 2012) and differentiation and virulence in *Leishmania major* (Smirlis *et al*., 2006). Despite the conservation of some functions, it remains unclear why H1 is dispensable for survival or growth of unicellular eukaryotes such as *S. cerevisiae* and *T. thermophila* (Shen *et al*., 1995; Shen and Gorovsky, 1996; Patterton *et al*., 1998; Fan *et al*., 2003), but is absolutely essential for mammalian embryonic development (Fan *et al*., 2003).

In *T. brucei*, H1 seems to be dispensable for growth in culture, but it is important to maintain *VSG* genes silent and to inhibit *VSG* switching during antigenic variation (Povelones *et al*., 2012). Like in other eukaryotes, H1 promotes chromatin condensation *in vitro* and *in vivo* (Burri *et al*., 1994; 1995). In this study we show that *T. brucei* H1 has a specific role in gene expression, by predominantly repressing Pol I transcription, namely of *VSG* and procyclin loci. Using labelling of nascent transcripts with 4-thiouridine (4sU), we show that H1 appears to act as a transcriptional inhibitor of *VSG* expression sites and procyclin loci. We further show that H1 inhibits DNA repair of methyl methanesulphonate (MMS)-induced lesions, indicating a role for H1 beyond transcriptional regulation. Finally, we show that although H1 seems to be dispensable for growth of parasites in culture, it is required for the rapid progression of an infection in mice, suggesting that regulation by this histone is important for the host–pathogen interactions.

Results

Depletion of H1 causes no considerable changes in parasite growth in culture

The current version of *T. brucei* genome (Berriman *et al*., 2005) indicates that there are five unique H1 genes on chromosome 11. As previously suggested (Grüter and Betschart, 2001), these genes are organized in two clusters belonging to a single polycistronic unit and are interspersed by 5 non-histone genes. We showed by PCR and Southern blot that this gene organization is correct in the *T. brucei* Lister 427 strain, although other H1 alleles may be missing from the genome database (Fig. S1). Since each gene is predicted to encode a unique protein, we assigned them paralogue numbers from H1.1 to H1.5 according to the most recent nomenclature for histone variants (Talbert *et al*., 2012) (Fig. 1A). Alignment of the five H1 protein sequences reveals that the first seven amino acids (a.a.) define three different types of N-terminal sequences (Fig. 1B). We classified them accordingly and named them MAKTT (H1.1), MAKASA (H1.2, H1.3 and H1.5) and MNNTT (H1.4). The sequence of the 3′UTRs is almost identical between H1 classes (96% on average), whereas the 5′UTRs are less conserved and specific for each of the three classes of H1 genes (Fig. S2).

To address the function of H1 in *T. brucei*, we generated RNA interference (RNAi) cell-lines that allowed simultaneous inducible depletion of all classes of H1. Because H1 genes are 89% identical, we expected that siRNAs generated from a dsRNA of a MAKASA gene (Alibu *et al*., 2005) would successfully knock-down all classes of H1 transcripts. Indeed, after inducing RNAi in two independent clones (C1 and C2), the mRNA levels of each of the three H1 classes (Fig. S3) were diminished to 39% on average during 6 days indicating that the knock-down was effective for all H1 classes in both clones (Fig. 1C, $P < 0.001$; Fig. S4A, $P < 0.001$). No significant differences in H1 depletion levels were observed between day 2, 4 and 6 of RNAi induction. The non-induced clones also showed a reduction of H1 transcripts (a decrease of 30% of the parental cell-line PL1S) (Fig. S4B), which is likely due to the previously described leaky expression of the RNAi

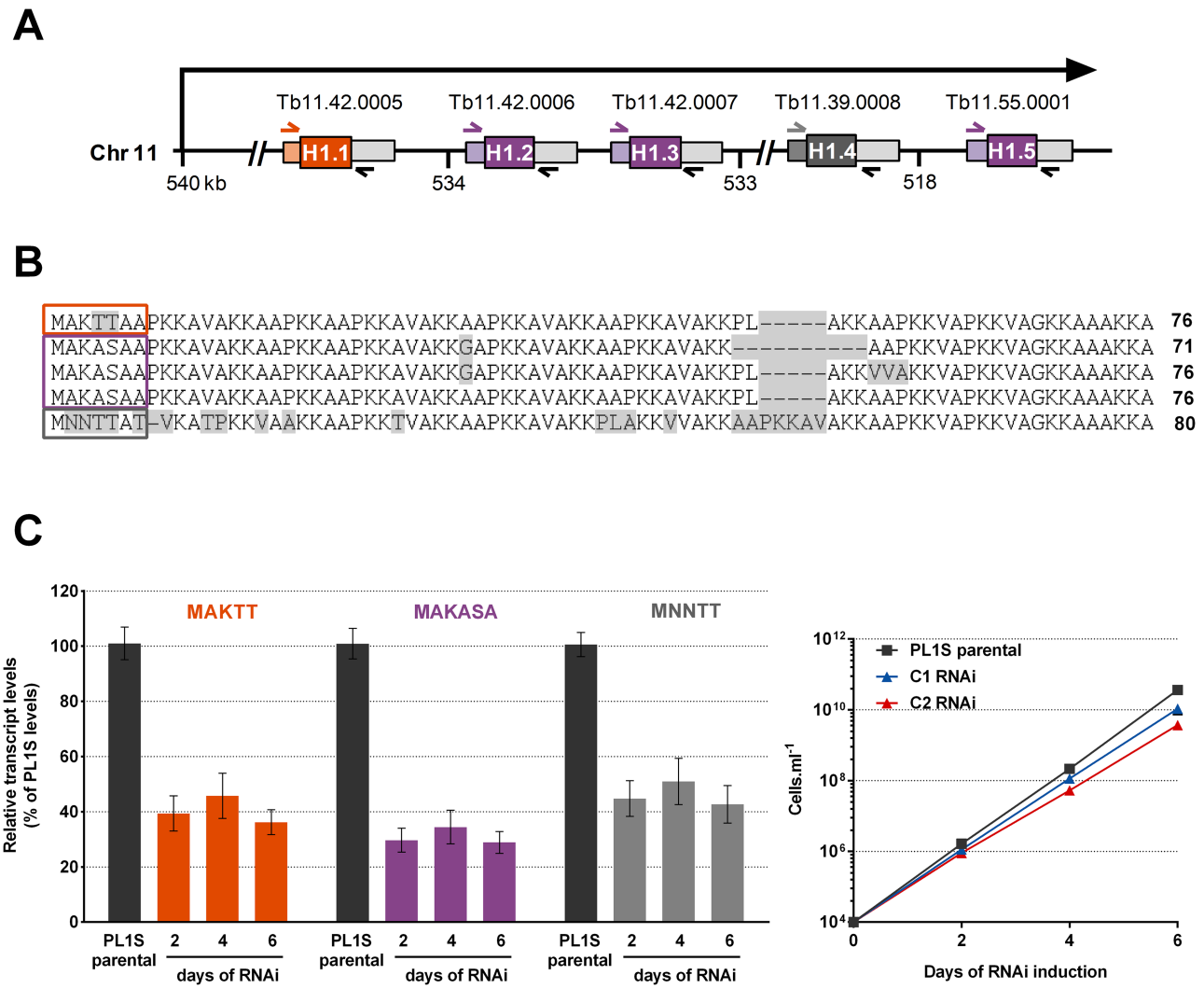

Fig. 1. Depletion of H1 leads to a subtle growth defect in culture.
A. Diagram shows that in *T. brucei* H1 gene family is encoded by five genes (H1.1-H1.5) in two clusters ~ 14.5 kb apart of the same polycistronic unit in chromosome 11. Arrow indicates the transcription start site and direction of transcription. Primers used for qPCR are indicated by colour-code: orange – primer specific for MAKTT 5′UTR; purple – primer specific for MAKASA 5′UTR; grey – primer specific for MNNTT 5′UTR; black – primers that anneal with the 3′UTRs, which are conserved across all H1 genes. Coding sequences are coloured according to the 5′UTR and N-terminal sequence (see panel B).
B. Alignment of the predicted amino acid (a.a.) sequences of H1 variants. Divergent a.a. are shadowed in grey. H1 variants were grouped into three classes according to the N-terminal sequences: MAKTT (orange), MAKASA (purple) and MNNTT (grey).
C. Efficiency of H1 depletion for each class during RNAi induction for 2, 4 and 6 days as an average of the two histone H1 RNAi clones relative to the parental cell-line PL1S. Transcript levels were measured by qPCR. Three independent experiments were analysed.
D. Growth in culture of BSFs of *T. brucei* upon H1 RNAi depletion during 2, 4 and 6 days. Five to nine independent experiments were analysed. Results are shown as mean ± SEM.

cassette (Alsford *et al.*, 2005). In induced clones we observed that depletion of H1 resulted in a minor growth defect *in vitro*. The doubling times were slightly longer in C1 (7:20 h) and C2 (7:40 h) compared with the parental cell-line PL1S (6:30 h) ($P < 0.01$) (Fig. 1D). This is consistent with previous observations (Povelones *et al.*, 2012). Although these mutants are not a complete knockout of the histone H1 gene family, our data suggest that H1 is not essential for growth of *T. brucei* in culture.

H1 compacts chromatin at different levels across the genome

It has been previously demonstrated, using *in vitro* systems, that *T. brucei* H1 can condense chromatin (Burri *et al.*, 1994; 1995). More recently, Povelones *et al.* used electron-microscopy analysis and micrococcal sensitivity assays to show that H1 plays a role in heterochromatin formation *in vivo*. Here we investigated the role of H1 in

chromatin condensation using an alternative approach: FAIRE (Formaldehyde-Assisted Isolation of Regulatory Elements) of H1-depleted clones subjected to RNAi induction for 6 days. By performing a phenol-chloroform extraction on a cross-linked and sheared chromatin sample, FAIRE fractionates DNA that is preferentially less tightly associated to proteins (such as histones) (Giresi *et al.*, 2007). Quantitative PCR (qPCR) was used to quantify such enrichment and a plasmid spike with an ampicillin-resistance gene (*AmpR*) was used as a normalizer for DNA input. Strikingly, silent BES promoter regions (97 bp downstream of transcription start site) were among the loci in which chromatin opened the most (Fig. 2). In both H1-depleted clones (C1 and C2), chromatin of the silent BES promoter regions opened on average 10-fold compared to the parental cell-line PL1S ($P < 0.001$) (Fig. 2B; Fig. S5A). The chromatin also opened at the luciferase gene (*LUC*), which is 1.2 kb downstream of a silent BES promoter, although in a slightly smaller degree (sevenfold relatively to PL1S; $P < 0.001$). In most other loci, loss of H1 resulted in a 1.8- to 4-fold increase in FAIRE enrichment (Fig. 2B), suggesting that chromatin becomes globally more accessible. These include silent *VSG*s from bloodstream and metacyclic expression sites (*VSG2*, *VSG3*, *VSG18*, *MVSG*; $P < 0.01$), the procyclin promoter region and procyclin *EP2* gene, typically transcribed in procyclic stages ($P < 0.01$), transcription start sites of RNA polymerase II (Pol II) polycistronic units containing either β-tubulin (*β-tub*-PR; $P < 0.01$) or structural maintenance of chromosome 3 gene (*SMC3*-PR; $P < 0.01$) and a number of Pol II-transcribed genes (very abundant *β-tub* and at lower levels *ISP*, *SMC3* and *PAG3*). Three loci showed a non-significant tendency for a more open chromatin conformation: the BES1 actively transcribed genes (blasticidin resistance gene, *BSD*^{R}, and *VSG9*) and the *18S* rDNA, all of which had been previously shown to have a very open, perhaps close to maximal, chromatin conformation (Figueiredo and Cross, 2010; Stanne and Rudenko, 2010).

The FAIRE results were further confirmed by chromatin immunoprecipitation (ChIP) of histone H3 (as a read out of nucleosome density). As previously shown (Figueiredo and Cross, 2010), FAIRE and H3 ChIP are highly consistent techniques and, globally, they reflect almost a mirror image from each other: for most loci, when chromatin becomes more open, we detect an increase in FAIRE-enrichment and a decrease in H3 ChIP for both clones (Fig. 2B–C and Fig. S5). A comparison between the *P*-values of FAIRE and H3 ChIP experiments further confirms the consistency of the two techniques (Table S1). We observe, by ChIP, that most genes lost around 30% of nucleosomes. As expected, ChIP revealed that silent BES promoters are the loci that, upon loss of histone H1, lost more histone H3 (close to 60%). Interestingly, although FAIRE did not detect a very dramatic change in chromatin condensation of the procyclin promoter region, H3 ChIP detected a reduction of nucleosomes more pronounced than average (48%). Also FAIRE did not detect a significant change in chromatin condensation of genes in active BES, but ChIP could detect a significant but modest loss of histone H3 at the promoter region but not at the active *VSG* gene. As expected, a gene encoded by the mitochondrial genome (cytochrome *c* oxidase subunit III, *COIII*, whose genome is not organized around nucleosomes), showed only background levels of histone H3 (Fig. S5B, $P > 0.05$). Overall, these results confirmed that when H1 is depleted there is a global loss of histone H3 across multiple loci of the genome, except for silent BES promoters, which opened 10-fold more (60% loss of histone H3) and procyclin promoters to a lesser extent. Moreover, our data greatly strengthen FAIRE as a robust method to study global changes in chromatin condensation.

H1 regulates expression of Pol I-transcribed genes

Given the global role of H1 in chromatin condensation, we next tested how changes in chromatin structure affected expression genome-wide. We used RNA-Seq to compare

Fig. 2. H1 compacts chromatin at different levels across genome.
A. Diagram indicates the amplicons (bars) amplified by qPCR for loci in BESs, procyclin loci, rDNA loci and a Pol II-transcribed polycistronic unit. Procyclin loci are partially transcribed in BSFs, as represented by a dashed arrow. Primers for EP2 procyclin are located in the 3′UTR (light grey).
B and C. Chromatin opening was measured by FAIRE (B) and nucleosome occupancy was determined by histone H3 chromatin immunoprecipitation (ChIP) (C) at several gene loci in parental cell-line PL1S and histone H1 RNAi clones 6 days after induction. DNA isolated by FAIRE was quantified by qPCR and an enrichment corresponds to a more open chromatin. An *AmpR* gene contained in a plasmid spike was used as a normalizer for DNA input. For H3 ChIP, DNA was quantified by qPCR, compared to the total input material and normalized to *18S* rDNA. Results are expressed as fold-change relatively to parental cell-line PL1S. Note that FAIRE enrichment is represented in a logarithmic scale. Data for individual clones prior to normalization to the parental PL1S are shown in Fig. S5. Significant fold-change ($P < 0.05$) is shown above (B) and below (C) dashed line in FAIRE and ChIP plots respectively. Two to three independent experiments were analysed. Results are shown in mean ± SEM. BSD^R, blasticidin resistance gene; VSG, variant surface glycoprotein gene; BES-P, promoter region of silent BESs; PUR^R, puromycin resistance gene; LUC, luciferase gene; MVSG, metacyclic VSG gene; Pro-P, procyclin promoter region; EP2, procyclin EP2 gene; rDNA-PR, rDNA promoter region; 18S, ribosomal *18S* gene; β-tub, β-tubulin gene; SMC3, structural maintenance of chromosome 3 gene; β-tub-PR, promoter region of β-tub polycistronic unit; SMC3-PR, promoter region of SMC3 polycistronic unit; ISP, inhibitor of serine peptidase gene; PAG3, procyclin associated gene 3.

the expression profile of H1-depleted clones (at day 4 of RNAi) and parental cell-line PL1S (Fig. 3, Fig. S6, Table S2). H1 depletion resulted in significant changes (false discovery rate (FDR) adjusted *P*-value < 0.05) in the expression of 26 out of 8996 expressed genes (Fig. 3A, Table S2). Interestingly, all were upregulated and all but one gene are transcribed by Pol I (Fig. 3A–C).

Most of these genes (18) are BES-associated genes (*VSG*s and *ESAG*s) or genes located in procyclin loci (EP procyclin genes and *PAG*s), which are normally silent in

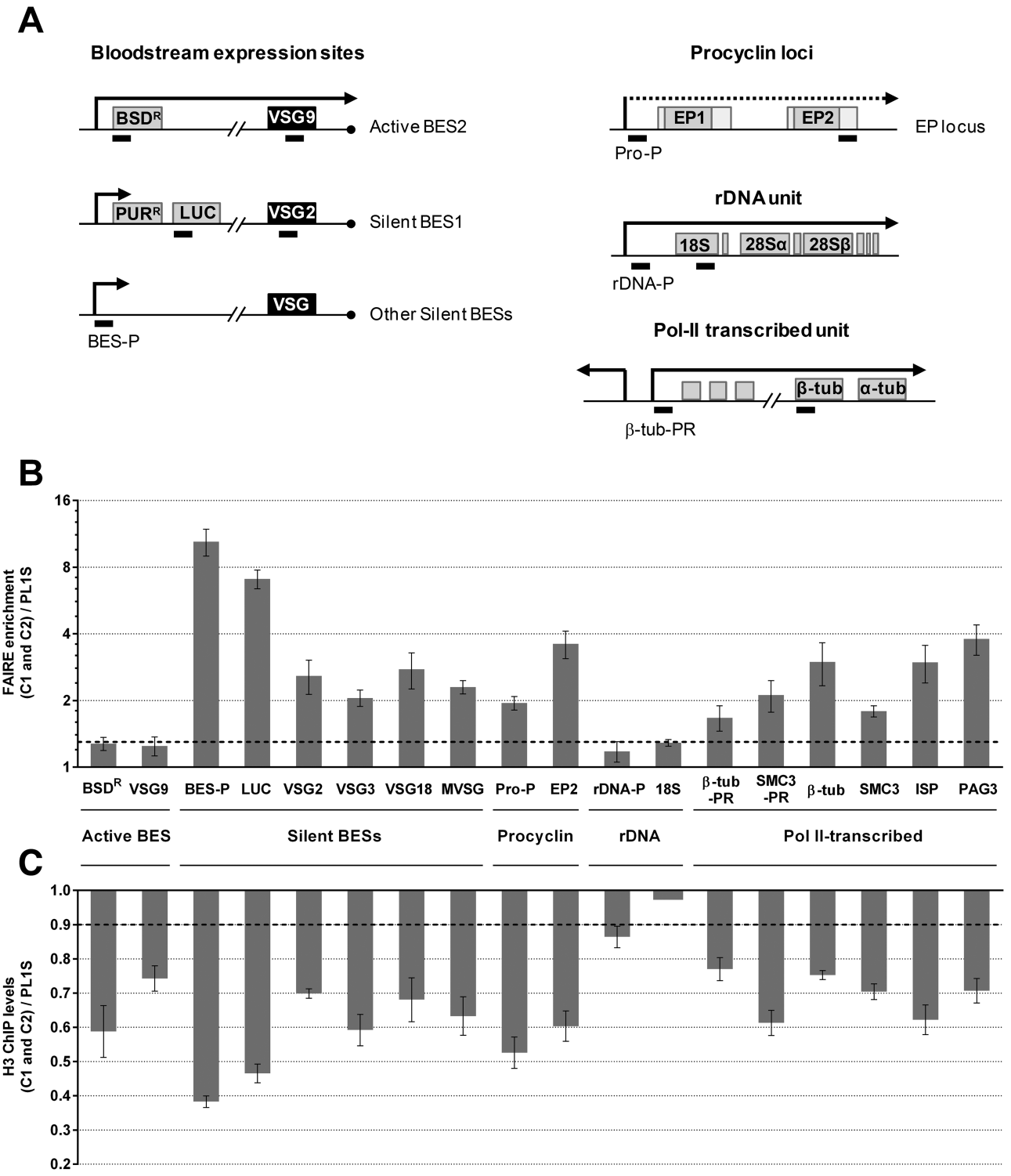

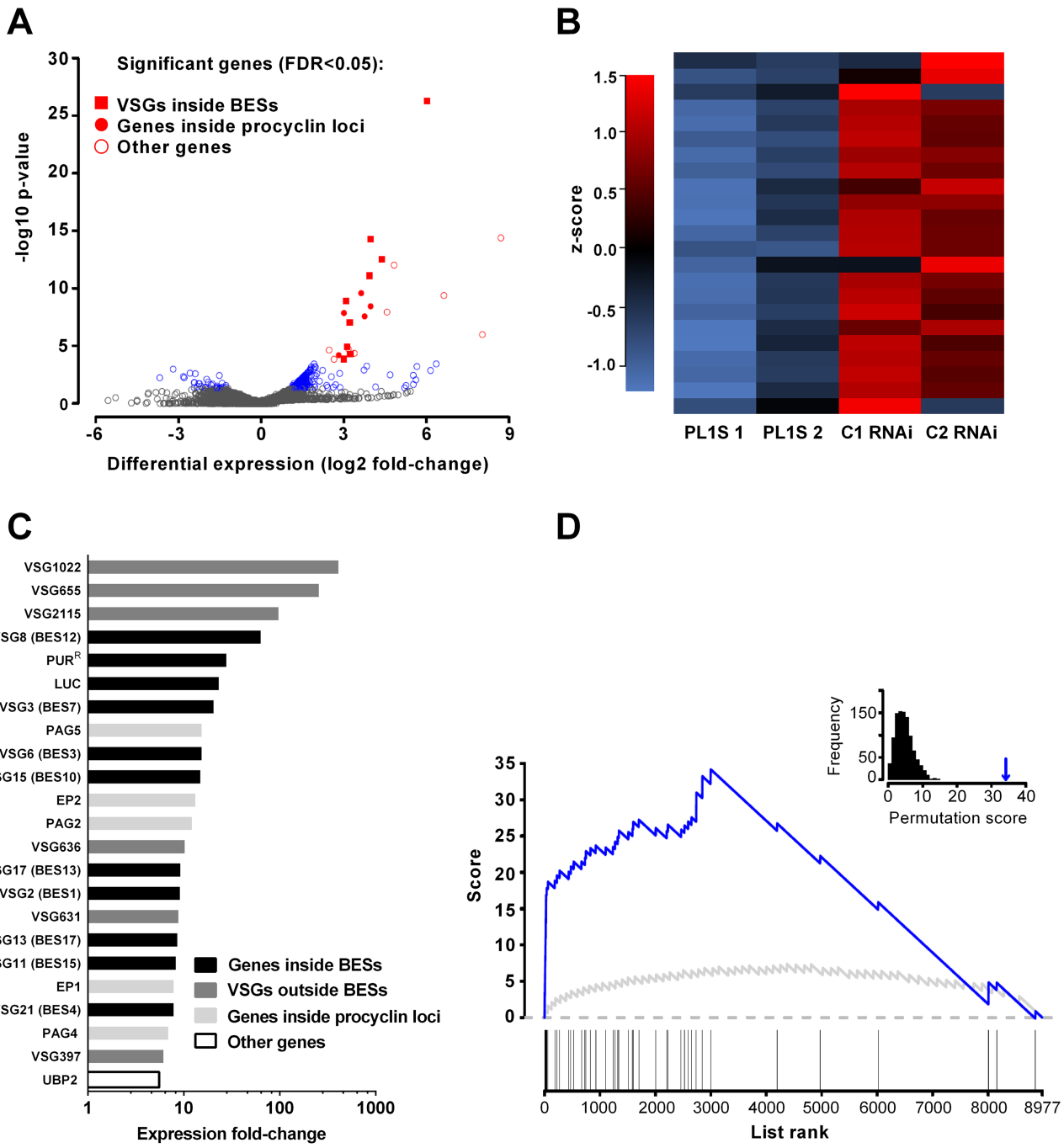

this stage of the parasite life cycle. In H1-depleted mutants, BES-associated *VSG*s are on average 18-fold more expressed, with a maximal derepression within this subset close to 65-fold (*VSG8*) (Fig. 3C, Table S2). Other eight *VSG*s annotated as outside a BES were also upregulated. Because we do not know the genomic location of these *VSG*s, we cannot evaluate whether there is a nearby promoter or polycistronic unit that could read through these *VSG*s. The transcript levels of 592 expressed *VSG*s did not change significantly, which is not surprising because in general *VSG* genes are located in tandem arrays that lack a functional promoter (Marcello and Barry, 2007). Most *VSG*s are not expressed and thus were not included in our analysis. H1 depletion also lead to an increased expression of the puromycin resistance (*PUR*^{R}) and the luciferase genes (Fig. 3C), both located immediately downstream of a silent BES promoter (BES1) (Fig. 2A), thus indicating that derepression

Fig. 3. H1 inhibits expression of RNA Pol I-transcribed genes. Genes with altered expression upon H1 depletion (4 days of RNAi) were identified by genome-wide RNA sequencing in BSFs of *T. brucei*.
A. Volcano plot analysis of differentially expressed genes between RNAi clones C1 and C2 relative to two biological replicates of the parental cell-line PL1S shows that H1 regulates a small set of genes, mainly located in procyclin loci (red filled circles) and bloodstream expression sites (BESs) (red filled squares). Each point represents a gene, with log2 fold-change (RNAi/PL1S) of gene expression across samples plotted on the *x*-axis and the corresponding statistical significance (–log10 *P*-value) plotted on the *y*-axis. Genes statistically significant (FDR-adjusted $P < 0.05$) are indicated in red; in grey are non-significant genes; in blue are those genes which would be significant if a less conservative statistical method had been used (FDR-adjusted $P > 0.05$ and $P < 0.05$).
B. Heatmap showing the *z*-scores calculated for the normalized DESeq expression levels of differentially expressed genes (FDR-adjusted $P < 0.05$) obtained by genome-wide RNA sequencing in BSFs of *T. brucei*. Genes are ordered by decreasing fold-change of expression, as in panel C.
C. Bar-plot showing the fold-change of expression of annotated differentially expressed genes in RNAi clones C1 and C2 relative to the parental cell-line PL1S. For *VSG* genes that are inside a BES, the respective BES number in shown in brackets.
D. Gene set enrichment analysis for genes located in BESs and procyclin loci. Blue line indicates the enrichment score distribution across genes ranked by decreasing statistical evidence of differential expression. Grey line represents 95th percentile of the enrichment scores obtained by 1000 random permutations of the gene ranks. The histogram at the top-right corner of the figure represents the distribution of maximum scores obtained by random permutation, with the arrow indicating the experimental enrichment score (i.e. the 'peak' in the main plot). The diagram at the bottom shows where the members of this gene set (i.e. genes located in BESs and procyclin loci) appear in the ranked list of genes. An FDR-adjusted $P < 0.001$ was obtained for this gene set, as described in *Experimental procedures*. Genes with undetermined fold-change due to too low unique read counts were excluded from the analysis.

occurred throughout the entire BES locus. However, as shown by the luciferase assay (Fig 4C), the derepression of silent BESs, is still far from the full activation seen in active BES, indicating that silent BESs are only partially derepressed. Only one of the *ESAG*s was found differentially expressed (*ESAG2* from BES12) most probably because the repetitive nature of *ESAG*s prevented unambiguous read alignment and were thus not included in the analysis. Due to too low unique read counts, the fold-change of *ESAG2* remained undetermined.

Although *PAG*s are located in multiple copies in the genome, in Pol II transcription units (Kim *et al*., 2013) or within the procyclin loci (Haenni *et al*., 2006), the differentially expressed members of *PAG2*, *PAG4* and *PAG5* are specifically located in these latter loci. For example, although there are two *PAG2* genes, one in the procyclin locus and the other in a polycistronic unit on the same chromosome 10, the only gene that is significantly upregulated when H1 is depleted is the one within the procyclin locus.

The results above strongly suggest that H1 predominantly inhibits expression of Pol I genes. We used gene set enrichment analysis (GSEA) (Subramanian *et al*., 2005) to investigate if specific gene sets are enriched or depleted among differentially expressed genes. We found that genes located in BESs and procyclin loci are very significantly enriched in our list of differentially expressed genes (FDR-adjusted $P < 0.001$), as illustrated by the large difference between the detected enrichment score distribution and the 95th percentile of the enrichment scores obtained by random permutations (blue and grey lines, respectively, in Fig. 3D) This enrichment is also observed if the two sets of genes are analysed independently (Fig. S7). This analysis further indicates that H1 plays an important role in the expression of Pol I-dependent genes.

RNA-Seq results were confirmed at the RNA level by qPCR (Fig. 4A–B; Fig. S8) and at the protein level by luciferase activity assay (Fig. 4C). First we checked the correlation between qPCR and RNA-Seq fold-changes of gene expression of 34 genes selected so that we would cover a wide range of expression levels. We observed a very high Pearson's correlation ($r = 0.90$) between the two types of experimental data, suggesting that qPCR and RNA-Seq are highly consistent (Fig. 4A). To further confirm the observation that Pol I, but not Pol II genes become derepressed when H1 is depleted, we measured by qPCR the transcript levels in the two RNAi clones induced for 2, 4 and 6 days (Fig. 4B, Fig. S9). These were normalized to *18S* transcript levels because these are highly expressed genes, depleted of H1 (Povelones *et al*., 2012) and with chromatin largely insensitive to H1 depletion (Fig. 2B). We confirmed that H1 depletion did not affect any of the tested Pol II transcribed genes nor the actively transcribed *VSG9*. As detected by RNA-Seq, *VSG*s in silent BESs (*VSG2* and *VSG3*) were significantly derepressed ($P < 0.001$) (Fig. 4B), although the level of derepression was slightly smaller by qPCR (5- to 12-fold) than RNA-Seq (9- to 21-fold). We also confirmed that procyclin *EP2* was fivefold derepressed. Another *VSG* in a silent BES (*VSG18*) and a *VSG* from a metacyclic expression site (*MVSG*) were found to be four- to fivefold derepressed by qPCR ($P < 0.001$) but were not detected as being differentially expressed in the RNA-Seq data. This inconsistency might be due to the fact that silent *VSG*s and *MVSG*s are expressed at a very low level in bloodstream forms (Donelson, 2003) and for this type of genes, statistical tests for differential expression based on RNA-Seq data are not very powerful.

Finally, BES derepression was further confirmed at the protein level by measuring the activity of luciferase in the

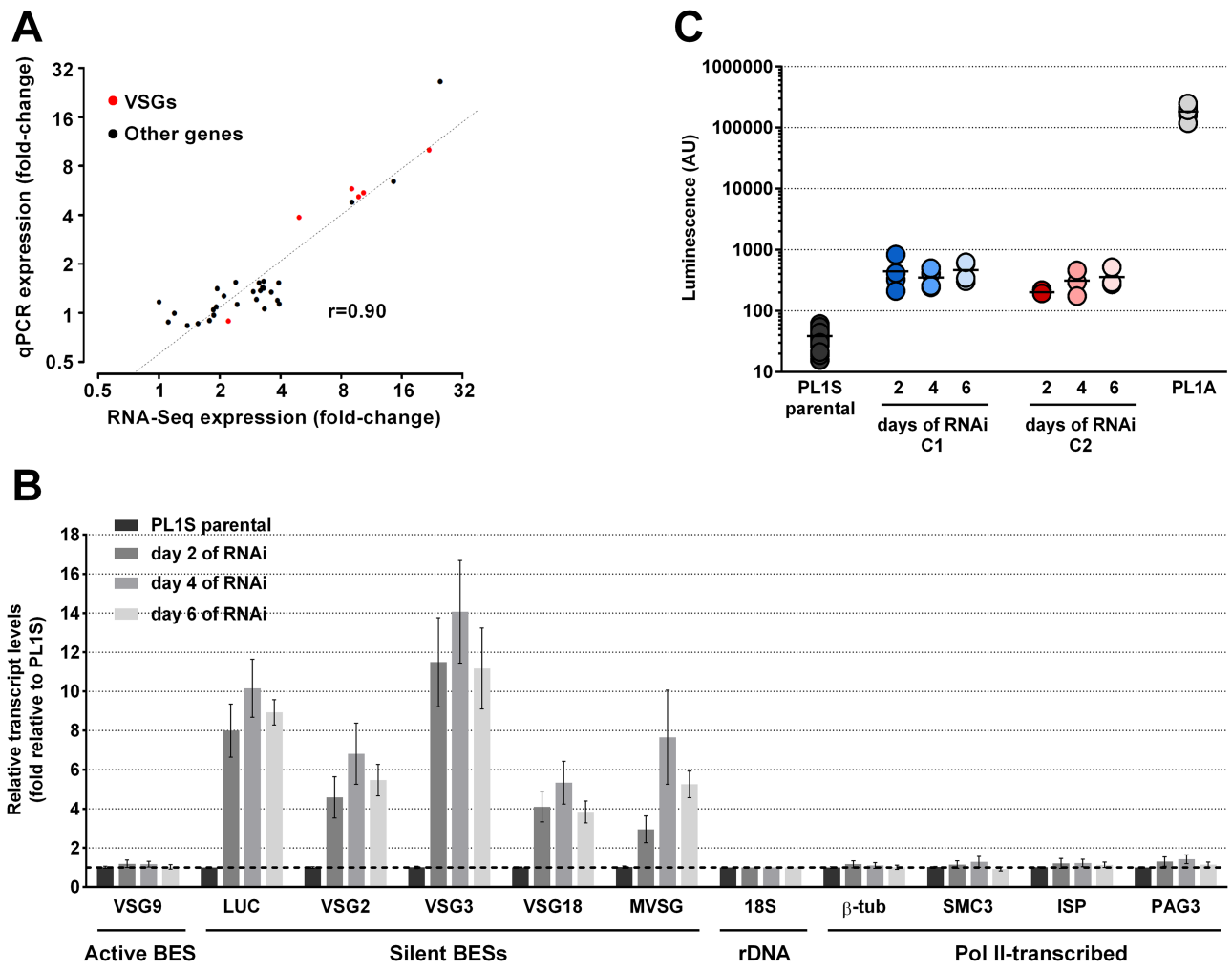

Fig. 4. RNA-Seq data are validated by qPCR and luciferase assays.
A. Scatter plot of fold-changes of gene expression in RNAi clones C1 and C2 relative to the parental cell-line PL1S. Thirty-four genes with mean expression levels ranging from 12 to 512,586 RPKMs by RNA-Seq were randomly selected and quantified by qPCR. Pearson's correlation coefficients (*r*) are indicated.
B. Quantification of mRNA expression after 2, 4 and 6 days of RNAi induction. Transcript levels are plotted as fold-change of RNAi clones C1 and C2 relatively to the parental cell-line PL1S. Transcript levels were measured by qPCR. Three independent experiments were analysed. Results are shown as mean ± SEM.
C. Derepression of silent BESs was assessed by quantification of luminescence throughout 2, 4 and 6 days of RNAi induction. A luciferase reporter gene located downstream of the promoter of silent BES1 (see diagram Fig. 2A) allows the monitoring of its transcriptional activity by measuring the luminescence emitted (AU, arbitrary units). Three to four independent experiments were analysed. PL1A refers to a cell-line that is isogenic of PL1S, but in which BES1 is active and therefore luciferase gene is transcribed at maximal levels.

entire population. We observed an increase in luciferase activity of 7- to 10-fold ($P < 0.001$; Fig. 4C), thus confirming RNA-Seq and qPCR data that silent BES1 was derepressed ($P < 0.001$; Fig. 4B). Overall, qPCR and luciferase activity assays confirmed/validated the RNA-Seq data.

We conclude that, like in genome-wide studies in mammalian cells and yeast (Hellauer *et al.*, 2001; Fan *et al.*, 2005), *T. brucei* H1 is not a global transcription repressor. It rather regulates a particular subset of genes, by repressing expression of Pol I-dependent genes. It is clear that the most significant subgroup of genes that is derepressed are genes from BESs or procyclin loci, confirming that H1 is essential for keeping these specific loci fully silent.

H1 inhibits transcription from silent BESs and procyclin sites

We next sought to understand how H1 depletion leads to an increase of steady-state mRNA levels of the silent *VSG*s and procyclins. Because H1 depletion leads to a more relaxed chromatin at Pol I promoter regions (especially at the silent BES promoters), we hypothesized that the increase in mRNA levels resulted from an increase in

transcription rates at these loci. To test this hypothesis we used metabolic labelling of nascent transcripts with 4-thiouridine (4sU). This method allows the quantification of newly synthesized RNA in live cells, therefore the direct measurement of RNA transcription rates with minimal interference on gene expression and cell viability (Dolken *et al*., 2008). After incubating *T. brucei* BSF parasites with 4sU, total RNA was extracted, thiol-specific biotinylated and subsequently purified on streptavidin-coated magnetic beads. qPCR was then used to quantify the newly transcribed RNAs purified.

We analysed the kinetics of 4sU incorporation into RNA in *T. brucei* during 2, 5, and 10 min of labelling. Since newly transcribed RNA contains higher amounts of unprocessed, primary transcripts, we determined the levels of nascent transcripts by quantifying the ratio of intergenic relative to coding sequence expression for *18S* and β-tubulin transcripts (Fig. 5A). As expected, we observed a rapid increase in the levels of 4sU-tagged RNA with increased duration of labelling (Fig. 5B). Based on this result and on previous reports (Rabani *et al*., 2011; Windhager *et al*., 2012), we chose 10 min as an appropriate 4sU-labelling time to estimate transcription rates. We next compared the levels of nascent transcripts of individual genes in a metabolically labelled sample relative to the total RNA. Although the yield of purification was generally low (0.015–0.025%), for all measured loci we observed that the labelled samples had 7- to 20-fold more nascent transcripts than non-labelled samples (Fig. 5C), indicating that the levels of labelled transcripts are significantly enriched over the background.

To test if the 4sU-labelled RNAs are a product of transcription, we repeated the labelling experiment in cells that were previously treated for 5 min with actinomycin D (ActD), a well-known transcription inhibitor. We observed that, upon transcription inhibition, the levels of 4sU-labelled RNAs recovered by MACS were dramatically reduced to the same low levels detected in the NO 4sU samples (Fig. 5D). Altogether these results further confirmed that 4sU-labelled RNAs are a reflection of the transcription happening inside live parasites.

4sU metabolic labelling was next used to test whether H1 depletion results in a higher transcription rate from BESs and procyclin promoters. For this, RNAi was first induced for 2 days in clones C1 and C2 and, at the end of this period, RNAi clones and parental PL1S parasites were incubated with 4sU. After 10 min the 4sU-labelling reaction was stopped and total RNA was extracted. The relative abundance of intergenic transcripts for *18S* and β-tubulin genes showed that purification of newly transcribed RNA was equally efficient in all cell-lines (Fig. 5E). Analysis of newly transcribed RNA revealed that H1 depletion indeed increases the transcription rate from silent BES promoters, resulting in higher abundance of precursor transcripts from the BES promoter region *BES-P* ($P < 0.001$) and the downstream luciferase gene ($P < 0.001$). When H1 is depleted, transcription rate is also higher from procyclin promoters, since we detected significantly more nascent transcripts from the procyclin promoter region ($P < 0.01$) and at the EP2 procyclin gene ($P < 0.001$) (Fig. 5F). These results show that when H1 is depleted, there seems to be a higher transcription rate of silent BESs and procyclin loci, most likely due to an increase of transcription initiation from the promoter. A Pol II gene (β-tubulin) showed no change in transcription rate, confirming the qPCR analysis of steady-state RNA levels (Fig. 4B). Curiously, the BES promoter regions are the loci in which the levels of nascent transcripts have increased the most (sixfold), which is consistent with the fact that the most dramatic changes in chromatin condensation observed upon H1 depletion were at the silent BES promoters. This may suggest a more significant role for H1 at silent BESs. We also observed a slight increase in transcription rate at the BSD^R gene located downstream of the active BES promoter, consistent with the decrease in H3 detected by ChIP. Taken together, these results not only support our RNA-Seq data but provide additional mechanistic insight, showing that histone H1 is an effective regulator of transcription at the Pol I-transcribed BESs and procyclin loci.

Depletion of H1 increases resistance to MMS-induced DNA damage

The fact that H1 is required for global chromatin compaction, but it has a very limited role in global transcription regulation, led us to hypothesize that H1 may play other functions in the cell. Povelones *et al*. have recently shown that H1 inhibits recombination of telomeric *VSG* genes, but not of a reporter gene *URA3* (Povelones *et al*., 2012). In yeast, H1 suppresses homologous recombination (HR) thus inhibiting DNA repair and promoting genome stability (Downs *et al*., 2003). To test if DNA repair is affected in *T. brucei*, we treated H1-depleted clones with a DNA-damaging agent, methyl methanesulphonate (MMS), and measured the subsequent cell survival. MMS is an alkylating agent that stalls replication forks, which are repaired by homologous recombination (Lundin *et al*., 2005). Parasites in log-phase growth were exposed to MMS for 2 days, after which cell viability was measured with Alamar Blue®. RNAi induction started 2 days before MMS treatment and continued throughout MMS exposure. We observed that both H1-depleted clones were clearly more resistant to MMS-damage than the parental cell-line PL1S (Fig. 6A). IC50 determined from dose–response curve was on average 2.76 parts per million (ppm) for PL1S and significantly higher for C1 and C2, 4.45 and 4.59 ppm respectively ($P < 0.01$) (Fig. 6B). This result indicates that DNA repair is more effective when H1 levels are reduced.

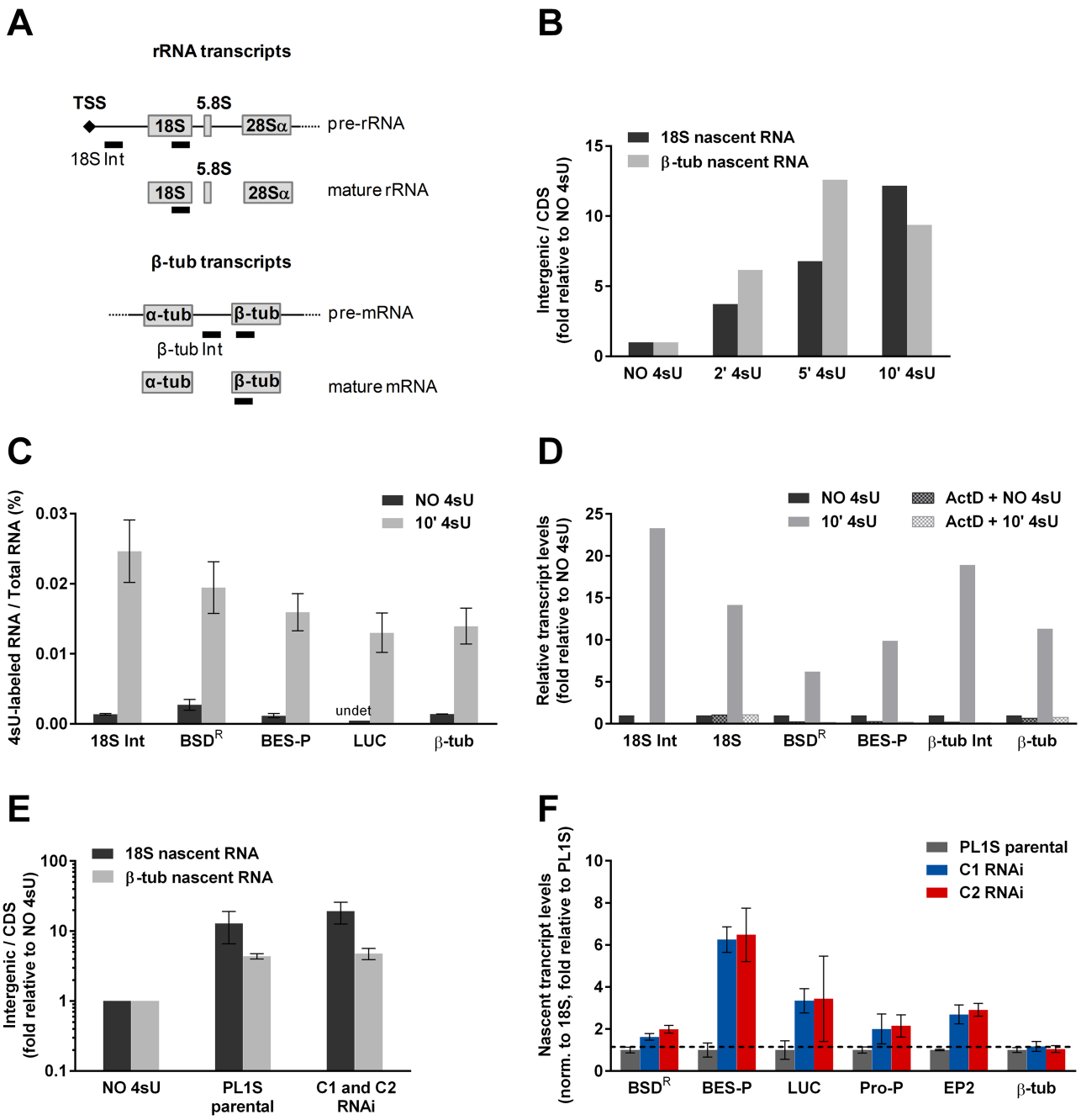

Fig. 5. H1 depletion results in increased transcription rate in silent BESs and procyclin loci. Nascent transcripts were labelled with 4sU for 10 min, biotinylated and streptavidin-purified. RNAs were quantified by qPCR, compared with non-labelled sample and normalized to *18S* rRNA transcripts.

A. Diagram indicates the amplicons (bars) amplified by qPCR for precursor and mature rRNA and β-tubulin transcripts.

B. Kinetics of 4sU-labelling of newly transcribed RNA measured by the ratio of intergenic/CDS transcripts.

C. Percentage of 4sU-labelled RNA relative to Total RNA for several loci with 10 min of 4sU-labelling.

D. Relative transcript levels in 4sU-labelled RNA in the absence or presence of a 5 min treatment with actinomycin D, which inhibits transcription, prior to 4sU-labelling for 10 min.

E. Enrichment in nascent transcripts in PL1S and H1-depleted mutants with 10 min of 4sU-labelling.

F. Fold increase in nascent transcripts in H1-depleted mutants in comparison with PL1S parental cell-line. Significant fold-change ($P < 0.05$) was calculated using an empirical Bayes approach and is shown above dashed line. Two independent experiments were performed; $n = 3–4$ for each cell-line.

Results are shown as mean ± SEM. Primers used to amplify 18S Int were the same used to amplify downstream promoter region of rDNA (rRNA-P). 18S Int, 18S intergenic region; β-tub Int, β-tubulin intergenic region; TSS, transcription start site.

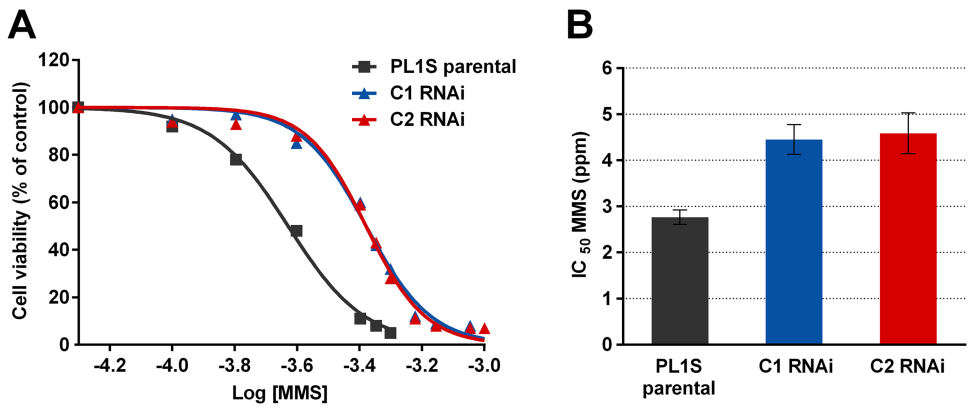

Fig. 6. H1 depletion increases resistance to MMS-induced DNA damage.
A. Dose–response curves of BSF of *T. brucei* to exposure to MMS, in parental and H1-depleted clones. Curves were obtained by fitting a non-linear regression with variable slope to the data. Cell viability was assessed by AlamarBlue® staining at the end of the treatment.
B. IC50 values calculated from the regressions. MMS concentration is expressed in parts per million (ppm) of volume. Seven to five independent experiments were analysed. Results are expressed in mean ± SEM.

This could be because H1 limits access to DNA repair machinery and, as a result, suppresses homologous recombination.

H1 is important for parasite fitness in vivo

Given the involvement of *T. brucei* H1 in DNA repair, *VSG* transcription and global chromatin condensation, it is surprising how H1-depleted parasites can grow so well in culture. Next, we investigated the impact of H1 depletion during an infection in mice. We inoculated C57BL/6 mice with 100 parasites of the parental cell-line, PL1S, or H1-depleted clones. In the latter, RNAi was pre-induced for 2 days with tetracycline. As previously published, mice also received doxycycline, a tetracycline analogue, in water 2 days before infection and during entire infection (Lecordier *et al.*, 2005). Doxycycline had no effect on PL1S-infected mice (Fig. S10A). Interestingly, mice infected with H1-depleted parasites survived longer ($P < 0.01$) (Fig. 7A). Indeed, whereas 55% of the PL1S-infected mice died in the first 9 days of infection, the majority of C1 or C2-infected mice survived until day 13 and 15, respectively. Such prolonged life-span was associated with a delay in parasite appearance in the blood (Fig. 7B; Fig. S11). In fact, whereas parental parasites reached detectable parasitaemia within 4–7 days of infection, H1-depleted clones took 4–15 days. This is much later than what would be expected from the growth delay measured *in vitro* (detectable parasitaemia should be reached at day 4–5), which indicates that host factors must have contributed to this diminished parasitaemia. It is interesting to note that the least virulent clone (C2) was the one with the most efficient H1 depletion ($P < 0.05$; Fig. 7A–C), suggestive of a dose-dependent response. Consistent with the fact that in 'non-induced' RNAi clones H1 transcripts are in fact 20% lower than in parental strain (Fig. S4B), in mice we observed that these clones caused a slight increase in life-span ($P < 0.01$) (Fig. S10B–C). These results clearly indicate that although H1-depleted cells have hardly any growth defect *in vitro*, H1 is essential for parasite fitness *in vivo*.

In around 50% of the mice infected with the parental cell-line PL1S and 40–75% of the mice infected with H1-depleted clones, two peaks of parasitaemia were detected (Fig. 7B; Fig. S11). In order to test if parasites detected in the second peak of H1-depleted clones were RNAi revertants, i.e. parasites that have lost the capacity of performing RNAi, we measured by qPCR the H1 transcript levels at 9–14 days post-infection. We observed that H1 transcripts were still reduced to around 40% and 12%, confirming that parasites were still depleted of H1 (Fig. 7C).

Typically in a *T. brucei* infection, parasites in the second peak of parasitaemia express a *VSG* different from the one expressed in the initially injected parasites. In order to confirm that VSG switching took place, we collected C1 and C2 parasites from the blood on days 9–14 post-infection and tested whether they were still expressing the original *VSG9* or if this *VSG* had become silent. By qPCR we confirmed that in H1-depleted parasites *VSG9* was no longer transcribed confirming that these mutant parasites had switched *VSG*s (Fig. 7 D). Overall, these results show that when H1 is depleted, parasite fitness becomes compromised but parasites are still capable of switching their *VSG*s.

Discussion

H1 condenses chromatin globally but has a more pronounced effect at silent Pol I transcription units

The ability of histone H1 to drive chromatin condensation has been demonstrated both *in vitro* (Thoma *et al.*, 1979;

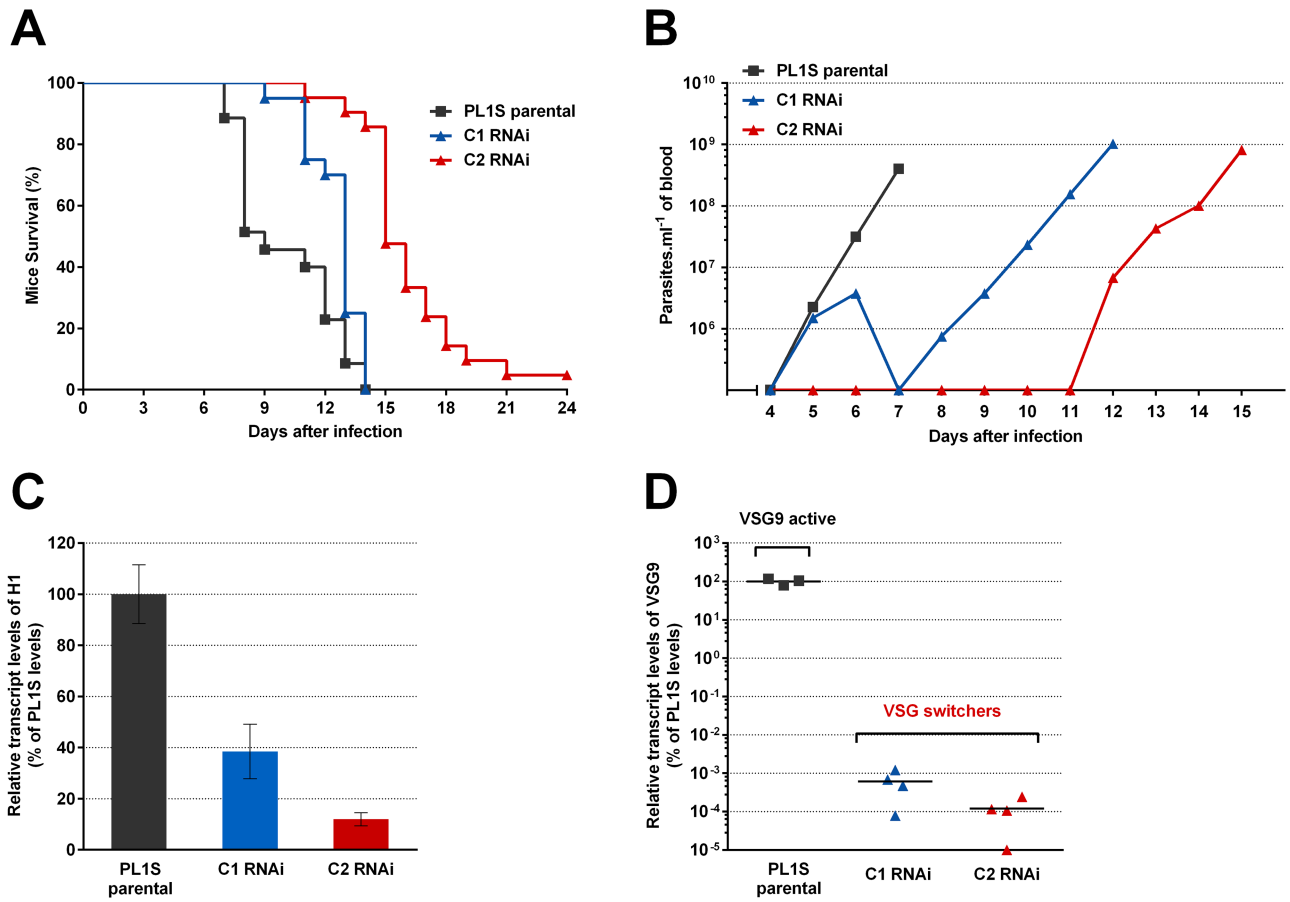

Fig. 7. H1 depletion compromises *T. brucei* fitness *in vivo*.
A. Survival of mice infected with 100 parasites of parental cell-line PL1S or the two H1-depleted clones (C1 or C2). Three to four independent experiments were analysed. Mice $n = 20–35$ per group.
B. Representative examples of parasitaemia in mice infected with *T. brucei* parasites depleted of H1. While PL1S parasites typically reached a peak in parasite number in 7–12 days, histone H1-depleted parasites had a delay of several days in parasitaemia.
C. Depletion of histone H1 in *T. brucei* parasites isolated from the blood of infected mice. PL1S parasites were collected at day 7 post-infection and C1 and C2 parasites at days 9–14 post-infection. Transcript levels of histone H1 were quantified with primers for all histone H1 classes by qPCR. Results are shown as percentage of transcript levels relative to PL1S levels.
D. Quantification of *VSG9* expression in parasites isolated from the blood of mice (same parasites analysed in (C)). C1 and C2 parasites underwent VSG switching and no longer express *VSG9*. Transcript levels were measured by qPCR. Mice $n = 3–4$ per group. Results are shown as mean ± SEM.

Burri *et al.*, 1994; 1995; Bednar *et al.*, 1998) and *in vivo* (Fan *et al.*, 2005; Masina *et al.*, 2007; Hashimoto *et al.*, 2010; Povelones *et al.*, 2012) for *T. brucei* and several other eukaryotes using multiple experimental assays. Using FAIRE and ChIP of H3, we showed here that depletion of H1 resulted in a global increase of chromatin accessibility (2.9-fold) and a 36% reduction of histone H3 of most loci, suggesting that H1 maintains chromatin compacted throughout the genome (Fig. 2B–C). The first exception to this rule is the actively transcribed *VSG* and *BSD*^{R} genes (BES1) and *rDNA 18S* gene, which probably already have a maximal chromatin decompaction and therefore chromatin remained essentially open in the presence of normal or reduced levels of H1. The most important exception to this general trend was the chromatin of silent BES promoters, which became 10-fold more open and lost more than 60% of histone H3. Procyclin promoter regions showed an average decompaction by FAIRE, but a significant drop in H3 content (48%), suggesting that the chromatin of these loci is also relatively sensitive to H1 loss. A similar trend was observed by Povelones *et al.* (2012) using an MNase sensitivity assay. Chromatin immunoprecipitation showed that silent BES promoters have more H1 than procyclin promoters (Povelones *et al.*, 2012), which may explain why depletion of H1 results in a more dramatic chromatin opening at the silent BESs than procyclin promoter regions. We conclude that, although *T. brucei* H1 has a global role in chromatin condensation, there are genomic sites, such as the BES promoters, in which H1 role seems to be more important or less redundant.

Consistent with an important function of H1 in the chromatin of BESs and somewhat procyclin promoter regions, almost all derepressed genes identified by RNA-Seq are from Pol I loci (*VSG*s, procyclins and *PAGs*) (Fig. 3D). It should be noted that rRNA genes, although transcribed by Pol I, were not included in our analysis due to their repetitive nature. How does histone H1 actually affect Pol I gene expression? To test if H1 acts at the transcriptional level, we chose to measure transcription rate by metabolically labelling nascent transcripts with 4sU nucleoside analogue. The advantage of this approach over the classic Nuclear Run-On is that the assay is done in unperturbed cells, instead of permeabilized cells or isolated nuclei. Despite a low yield of recovery, we clearly show that a 4sU-labelled RNA sample is enriched in molecules of RNA that contain intergenic sequences, which are present in primary, unprocessed transcripts (so-called nascent transcripts). Moreover, we showed that 4sU-labelling is dependent on transcription, suggesting that the transcript levels in 4sU-labelled RNAs are a reflection of transcription rates of these genes. Using this metabolic labelling, we observed that depletion of H1 apparently leads to an increased transcription rate of silent procyclin loci and BESs, but no changes in transcription of Pol II loci (Fig. 5). Because we detected BESs derepression with a pair of primers located immediately downstream of the BESs silent promoters, we can conclude that H1 acts at least in part as an inhibitor of transcription initiation. These results are consistent with a recently published work that showed that BES monoallelic transcription is controlled at least partially at the level of transcription initiation, which is dependent on the CITFA complex (Nguyen *et al*., 2014). To our knowledge this is the first mechanistic evidence in *T. brucei* on how depletion of a chromatin component results in an increase of steady-state transcripts by increasing transcription rate, particularly at BESs.

It is interesting to notice that, upon H1 depletion, the FAIRE analysis revealed that chromatin of a silent BES opened 10-fold at the promoter, 7-fold at the luciferase gene (1.2 kb downstream of BES promoter) and 2.6-fold at *VSG2* (56.4 kb downstream BES promoter). Such gradual decreasing effect of chromatin decompaction with increasing proximity to telomeres was also detected by H3 ChIP and it suggests that changes in chromatin is not homogeneous throughout the entire BES. These chromatin changes are also reflected at the RNA level, since a gene close to the promoter of BES1 (Luciferase) was more derepressed than VSG2, which is at the telomeric end of the same BES (Fig. 4A and RNA-Seq, data not shown). Such disparities of derepression at the beginning and end of a silent BES have been observed in other mutants, namely in mutants for TbISWI, TbSPT16, TbDAC3 and TbNLP, in which the BES promoter region was derepressed, but not *VSG*s (Hughes *et al*., 2007; Denninger *et al*., 2010; Wang *et al*., 2010; Narayanan *et al*., 2011). In contrast, deletion of TbRAP1 and TbMCM-BP resulted in a stronger derepression of VSG genes than silent BES promoters (Yang *et al*., 2009; Kim *et al*., 2013). Although it is not clear how these factors interact with each other to regulate VSG expression, these studies are in agreement with previously described silencing mechanisms, which act either at transcription elongation level (Vanhamme *et al*., 2000) or emanate from telomeric silencing (Yang *et al*., 2009). In this context, we propose that histone H1 helps maintaining a compact chromatin structure throughout silent BESs, but with a predominant role at the promoter regions. When H1 is depleted, chromatin of silent BES promoter regions opens dramatically, facilitating transcription initiation by RNA polymerase I. At the telomeric end of BESs, H1 depletion also leads to opening of chromatin but not so dramatically, thus inhibiting transcription elongation. Most likely, the same mechanism happens at procyclin loci.

Although depletion of H1 caused global changes in chromatin condensation, the number of genes with significantly altered expression levels was low (only 26 out of 8996 expressed genes). Similar trends have been observed in the past: only 26 of over 6000 genes were downregulated in H1 knockout mutants of yeast, (Hellauer *et al*., 2001); and 29 genes in mammalian cells showed an altered expression of more than twofold (Fan *et al*., 2005). In contrast to these organisms, however, *T. brucei* H1 acts only as a negative-regulator of gene expression, since H1 depletion results in higher transcripts levels for all significant genes. We conclude that (i) H1 is not a global regulator of gene expression in *T. brucei*, (ii) H1 predominantly represses transcription of silent Pol I genes, and (iii) H1 inhibits at least in part transcription initiation from silent BESs. These specific roles of histone H1 in Pol I loci is likely due to the fact that Pol I genes are probably the only ones that are transcriptionally regulated in *T. brucei*. In fact, because most Pol II-dependent genes are organized in polycistronic units, their expression is believed to be constitutive and gene regulation of Pol II to occur mainly post-transcriptionally.

H1 plays a role in DNA repair

It is interesting to notice that the discrepancy between a global role of H1 in chromatin compaction and the limited role in transcription regulation has also been observed in other organisms (Hellauer *et al*., 2001; Fan *et al*., 2005). It is therefore likely that *T. brucei* H1 plays important but yet unsolved roles that go beyond transcription regulation. Indeed, in *T. brucei*, as in *S. cerevisiae* (Downs *et al*., 2003), H1 is inhibitory of DNA repair (Fig. 6). This could be due to the role of H1 in keeping chromatin closed and thus

refractory to DNA repair machinery. These results are also consistent with the observations that H1-depleted cells undergo more frequent *VSG* gene conversion, a recombination-based switching mechanism (Povelones *et al*., 2012).

H1 depletion showed no changes of parasite growth in culture but revealed important differences of parasite fitness in vivo

In *T. brucei*, when 61% of H1 is depleted by RNA interference a modest defect on cell growth was observed for cultivated bloodstream parasites (Fig. 1 D) (Povelones *et al*., 2012). This suggests that, like other lower eukaryotes, H1 may not be essential for *T. brucei* survival in culture. An alternative explanation is that the remaining H1 (20–30%) is sufficient for *T. brucei* survival. When we infected mice with H1-depleted parasites, these mutant parasites were substantially less infective, allowing mice to survive up to twice longer (Fig. 7A–B). This is probably associated to the lower parasitaemia in the first days of infection. Why is parasitaemia lower in an infection with H1-depleted parasites? This cannot be simply explained by the slower parasite growth rate detected *in vitro*. Indeed, based on *in vitro* growth rate, we estimated a delay in parasitaemia of up to 1 day, but *in vivo* the delay ranged from 1 to 10 days, which indicates that H1 is necessary for adapting to the host environment at the onset of infection. Several mechanisms could explain the reduced fitness of H1-depleted parasites. First, it is possible that the simple deregulation of gene expression could have a negative impact on putative mechanisms that may allow Trypanosomes to sense and adapt to the host environment. These genes could be among the 26 differentially expressed genes, or other genes whose repetitive nature prevents unambiguous mapping of RNA-Seq reads and accurate expression analysis (ESAGs and rRNAs, for example). Consistent with this hypothesis, overexpression of H1 in *L. major* results in a delay in differentiation of promastigotes into amastigotes (Smirlis *et al*., 2006). Second, derepression of silent *VSG*s or increased *VSG* switching frequency may make the first peak of parasitaemia a heterogeneous one that is more easily controlled by the immune system. Indeed, Povelones *et al.* showed that deletion of H1 results in a slight increase in VSG switching (Povelones *et al*., 2012).

When a second population of parasites establishes (switchers) (Fig. 7D), parasitaemia increases very rapidly, eventually killing the mouse. One possible explanation for this rapid growth is that, after 9–14 days of infection, parasites have activated a compensatory pathway for H1 function, which could involve replacement by other small chromatin-interacting proteins such as High-Mobility Group proteins (Hill and Reeves, 1997).

In this work we showed that *T. brucei* H1 keeps chromatin globally compact, inhibits DNA repair and represses the transcription of Pol I silent genes, including *VSG*s and procyclins, which become around 15-fold derepressed on average. We showed that such derepression is associated to an opening of chromatin at silent BESs and silent procyclin loci, which likely results in the observed increase in transcription rate from both types of promoters. Our data show that H1 keeps chromatin of silent BES promoter and to a lesser extent chromatin of procyclin promoters in a condensed state, keeping transcription rate of these loci low. It would be interesting to determine if, in other organisms, histone H1 also acts as an inhibitor of Pol I transcription.

Experimental procedures

Cell-lines and growth medium

Trypanosoma brucei bloodstream-form (BSF) parasites (strain Lister 427, antigenic type MiTat 1.2, clone 221a) (Johnson and Cross, 1979) were cultured in HMI-11 as described in Hirumi and Hirumi (1989). PL1S cell-line was described in Yang *et al.* (2009). Cells were diluted according to their doubling times in order to maintain log-phase growth. Cell growth was measured by counting cells in a Neubauer chamber. H1 RNAi cell-line clones (C1 and C2) were obtained by transfecting *T. brucei* PL1S cells with a construct (pLF100i), p2T7TA RNAi vector in which a MAKASA H1 gene is under the inducible control of two opposing T7 promoters (Alibu *et al*., 2005). RNA interference (RNAi) was induced by adding 1 μg ml^{-1} of tetracyclin (Fisher Scientific) to the medium for a maximum of 6 days. Cloning was performed by recombination of PCR-amplified fragments using the In-Fusion® HD Cloning system (Clontech).

Real-time quantitative PCR analysis

Parasites were harvested by centrifugation at 650 *g* for 10 min, 4°C and immediately resuspended in PureZOL (Bio-Rad) or TRIzol (Invitrogen). RNA was isolated following the manufacturer's instructions and RNA quantity and quality was assessed on a NanoDrop 2000 (Thermo Scientific). The procedure used to isolate nascent RNA labelled with 4sU is described in a section below. cDNA was generated using a Superscript cDNA Synthesis Kit (Invitrogen), according to manufacturer's protocol. Quantitative PCR (qPCR) was performed using 1 × SYBR Green PCR Master Mix (Applied Biosystems). Negative controls lacking reverse transcriptase (RT-) were confirmed by qPCR. Primer efficiencies were determined using standard curves with 3-logs coverage. Amplification reactions were performed in duplicates. Relative quantification was performed based on the CT (cycle threshold) value and the PCR efficiency-corrected method of Pfaffl (Pfaffl, 2001). DNA and transcript levels were normalized to those of *18S*, which did not change significantly after histone H1 depletion. Primer sequences are listed in Table S3.

FAIRE

Formaldehyde-assisted isolation of regulatory elements (FAIRE) was adapted to *T. brucei* as described previously (Figueiredo and Cross, 2010). The main difference is that an external DNA spike consisting of the commercial vector pBluescript-SK (Promega) was added to the samples prior to sonication. Quantification of the FAIRE and total DNA samples was performed by real-time qPCR as described above.

Chromatin immunoprecipitation

Chromatin immunoprecipitation (ChIP) was performed essentially as described (Siegel *et al*., 2009). Histone H3 custom made antibodies were provided by Christian Janzen.

RNA-Seq data analysis

Total RNA was extracted 4 days after induction of H1 depletion *in vitro*. Ribosomal RNA was depleted with RiboMinus kit (Invitrogen). PolyA-containing RNA was purified using Dynabeads oligo-(dT) (Invitrogen) and cDNA was synthesized using random hexamers according to Complete RNA-seq Library System kit (NuGEN) instructions. Samples were sequenced in an Illumina HiSeq2000 platform (EMBL). Sequence reads were 100 nucleotides long and paired-ended. Their quality was accessed using the FASTQC quality control tool (http://www.bioinformatics.babraham.ac.uk/projects/fastqc/). Contiguous read segments for which the quality score at each base was greater than 28 (-h 28), and longer than 25 nucleotides (-l 25) were selected using the DynamicTrim and LengthSort Perl-based software respectively (Cock *et al*., 2010). The sequencing data were then aligned to a hybrid genome composed of the Tb927 genome (TriTrypDB v 4.1), in which the *VSG* coding regions in subtelomeric *VSG* arrays were removed and replaced with the Tb427 *VSG* coding regions as a separate chromosome. Alignments were obtained using bowtie 2 (Langmead *et al*., 2009), allowing for one mismatch. Non-unique reads (i.e. aligning in different locations) were excluded and the number of reads mapping to each feature (gene) was measured with the htseq-count software (http://www-huber.embl.de/users/anders/HTSeq/doc/count.html) using the 'intersection-strict' mode. These sequence data have been submitted to the ArrayExpress database (EBI-EMBL) under Accession No. E-MTAB-1715.

Differential gene expression was analysed in R (v 3.0.2), using DESeq (v 1.14.0) (Anders and Huber, 2010) from Bioconductor (v 2.6). DESeq uses the negative binomial distribution for modelling read counts per genomic feature. We first estimated the relative library sizes with the function estimateSizeFactors: for a matrix of raw read counts (where samples are represented in columns and genes in rows), each column is divided by the geometric means of the rows and the median of these ratios is used as the size factor for that specific column. Then, we used the function estimateDispersions: for each condition, it first computes an empirical distribution value for each gene, then fits by regression a dispersion-mean relationship and finally chooses for each gene, from the empirical and the fitted value, a dispersion parameter that will be used in subsequent tests. The function nbinomTest was finally used to test for differences between the base means of the two conditions (RNAi and PL1S in this case).

Feature regions were defined as gene coding sequence (CDS) regions, except in cases where the number of uniquely mappable positions inside the CDS is smaller than 100, in which case UTRs (annotated by Nilsson *et al*., 2010) were also included. To determine uniquely mappable positions we extracted all 100bp sequences (pseudo-reads) appearing in the reference genome and mapped them back using the same software and parameters used previously. After filtering out non-unique alignments, positions where one pseudo-read was successfully mapped were considered mappable. We corrected for multiple comparisons by controlling the FDR, following the Benjamini-Hochberg procedure (Benjamini and Hochberg, 1995), which relies on the *P*-values being uniformly distributed under the null hypothesis consists of sorting the *P*-values in ascending order, and then dividing each observed *P*-value by its percentile rank to get an estimated FDR (Noble, 2009). Genes with a FDR-adjusted *P*-value < 0.05 were considered significant.

Gene set enrichment analysis

Gene set enrichment analysis (GSEA) was performed as described in Subramanian *et al*. (2005). GSEA allows us to investigate if specific gene sets (i.e. groups of genes that share common biological properties of interest) show statistically significant, concordant differences between two biological states and are therefore correlated with the phenotypic distinction under study. Non-expressed genes were removed from the analysis and the remaining were ranked by differential expression *P*-value. For a given gene set S (in Fig. 3D 'Genes inside BESs and procyclin loci'; in Fig. S7 'Genes inside BESs', 'VSGs inside BESs', 'VSGs outside BESs' and 'Genes inside procyclin loci'), an enrichment score was calculated by walking down the ranked list of genes increasing a running-sum statistic when the gene is in S and decreasing it otherwise and extracting its maximum value at the end. Thus, a high enrichment score indicates a preference for the genes in S to be among the more significantly differentially expressed genes. Statistical significance of this enrichment was determined by comparing the observed maximum enrichment score for gene set S with the distribution of maximum scores obtained by randomly permuting the gene ranks 1000 times (histogram in the top right corner), allowing the estimate of the associated FDR-adjusted *P*-value. That significance is also illustrated by comparing the distribution of scores across observed gene ranks (blue line) with a simulation of scores distribution if gene ranks were randomly selected (grey line). This simulation was generated by 1000 random permutations of the gene ranks and represented as the 95th percentile of the enrichment scores obtained.

Luciferase activity

Luciferase activity was measured with a Firefly Luciferase Kit (Biotium) from 1.5×10^6 parasites following the manu-

facturer's protocol. Luminescence was measured in an Infinite M200 plate reader (Tecan).

4sU-labelling and purification of nascent transcripts

For metabolic labelling of newly transcribed RNA, 150–185 million bloodstream parasites were collected by centrifugation at 970 *g* for 10 min, at room temp. and, washed three times each with 25, 50 and 2 ml of trypanosome dilution buffer (TDB) (5 mM KCl, 80 mM NaCl, 1 mM $MgSO_4$, 20 mM Na_2HPO_4, 2 mM NaH_2PO_4, 20 mM glucose, pH 7.7). Cells were resuspended in 2 ml of TDB and 4-thiouridine (4sU) (Sigma) was added to a final concentration of 500 μM for 2, 5 or 10 min at 37°C. In experiments where transcription was inhibited, actinomycin D (Sigma) was added to a final concentration of 20 μg ml^{-1}, 5 min before starting 4sU-labelling. A negative control sample, with parasites with no 4sU addition (NO 4sU sample), was also included for each experiment. Total RNA was extracted using TRIzol reagent (Invitrogen) following the manufacturer's protocol and RNA was dissolved in RNase-free Tris-EDTA buffer (TE) (10 mM Tris-HCl pH 8, 1 mM EDTA). Sample quantity and quality was assessed in a NanoDrop2000 (Thermo Scientific). Biotinylation and purification of 4sU-labelled RNA was performed essentially as described before (Dolken *et al.*, 2008). Labelled RNA was biotinylated with EZ-Link Biotin-HPDP (Pierce), dissolved in dimethylformamide (DMF). Biotinylation reaction was carried out in labelling buffer (10 mM Tris-HCl pH 8, 1 mM EDTA) and 0.2 mg ml^{-1} Biotin-HPDP for 1.5 h at room temperature. An amount of 50–90 μg of total RNA was used for the biotinylation reaction. Unbound Biotin-HPDP was removed by chloroform/isoamyl alcohol (24:1) extraction. RNA was precipitated with a 1:10 volume of 5 M NaCl, an equal volume of isopropanol and 15 μg of GlicoBlue (Life Technologies) at 20000 *g* for 20 min, 4°C. The pellet was washed with an equal volume of 75% ethanol and resuspended in RNase-free TE. Biotinylated RNA was captured using μMACS streptavidin beads and columns (Miltenyi). Up to 58 μg of biotinylated RNA was incubated with 100 μl of beads for 15 min at room temperature, with rotation. Beads were magnetically fixed and washed 3× with washing buffer (100 mM Tris-HCl pH 7.5, 10 mM EDTA, 1 M NaCl, 0.1% Tween20) at 65°C followed by 3× washes with washing buffer at room temperature. 4sU-labelled RNA was eluted in two rounds by adding 100 μl of freshly prepared 100 mM dithiothreitol (DTT). Eluted RNA was precipitated with a 1:10 volume of 5 M NaCl, 2.5× volume of 100% ethanol and 30 μg of GlicoBlue, at –80°C for at least 30 min. RNA was washed in 75% ethanol and recovered by centrifugation as described above and resuspended in RNase-free water. cDNA synthesis and qPCR analysis was performed as described in a previous section. Levels of nascent transcripts were assessed by calculating the ratio of intergenic/CDS levels for *18S* and *β-tub*. In this case, an internal normalization for *18S* was not needed since two types of transcripts are being compared inside the same sample. The fold-change relative to NO 4sU samples was then calculated and plotted. In the experiment where transcription was blocked by actinomycin D treatment, an equal amount of RNA was used to synthesize cDNA and no further normalization was applied. Transcript levels for each locus in the MACS-isolated fraction were plotted as fold-change to the NO 4sU sample. To compare nascent transcript levels in H1 RNAi clones relative to PL1S, qPCR levels were first normalized to those of *18S* transcripts and afterwards fold-change was calculated for H1 RNAi clones at each locus, relative to its expression in PL1S.

MMS-induced DNA damage

Parasites in which RNAi has been pre-induced for 2 days with tetracycline (1 μg ml^{-1}), were incubated in a 96-well plate (200 μl per well) with sixfold range dilutions of methyl methanesulphonate (MMS; Sigma) in HMI-11, at a final concentration of 0.5–4 × 10^4 cells ml^{-1}. After 2 days, cell viability was measured with AlamarBlue® (Sigma). Ten microlitres of Alamar Blue® was added per well followed by incubation at 37°C, 4 h and fluorescence was measured (530ex/590em nm). RNAi induction with tetracycline and selection with Hygromycin was maintained during the 2-day exposure to MMS. MMS concentration is expressed in parts per million (ppm) of volume.

Mouse infections

Inbred C57BL/6 wild-type mice (Charles River) were housed in the pathogen-free facilities of the Instituto de Medicina Molecular (IMM). The animal facility and the experimental procedures complied with European Guideline 86/609/EC, followed the Federation of European Laboratory Animal Science Associations (FELASA) guidelines and recommendations concerning laboratory animal welfare and were approved by the Instituto de Medicina Molecular Animal Care and Ethics Committee (AEC_2011_006_LF_TBrucei _IMM). Mice were infected intraperitoneally with 100 parasites of *T. brucei* Lister 427 PL1S and RNAi clones C1 and C2 (with and without induction). RNAi induction was initiated in culture with 1 μg ml^{-1} tetracycline 2 days prior to mouse infection. RNAi was maintained *in vivo* in mice by watering them with 1 mg ml^{-1} of doxycycline (doxycycline hyclate, Sigma). Mice received doxycycline 2 days prior to infection and during the whole course of infection. Parasitaemia was monitored throughout infection by collecting blood from the mouse tail. For RNA extraction of parasites in the blood, between day 7 and 14 post-infection, 25–30 μl of blood from the tail of infected mice (parasitaemia ~10^8 parasites ml^{-1} of blood) was collected in red blood cell lysis buffer (150 mM NH_4Cl, 10 mM $KHCO_3$, 1 mM EDTA.Na_2, pH 7.4), washed in 1× TDB and extracted with PureZOL, according to manufacturer's instructions (Bio-Rad). cDNA synthesis and qPCR were performed as described above.

Statistical analysis

To estimate statistical significance of data calculated as a fold increase, we computed a log-normal posterior distribution of the fold-change, using an empirical Bayes approach (FAIRE, ChIP and 4sU experiments). Survival curves were compared by a Log-rank (Mantel-Cox) test. The statistical significance for remaining comparisons was given by Mann–Whitney *U* tests. A *P*-value < 0.05 was considered significant. For the statistical analysis of RNA-Seq data, see RNA-Seq methods above.

Acknowledgements

The authors thank all members of the Parasitology group at IMM and the Lisbon Chromatin Club for helpful discussions; George A.M. Cross for allowing L.M.F. to begin some preliminary experiments during her post-doc, for sequence information on VSGnome, and for critically reading the manuscript; Christian Janzen for the generous gift of H3 antibody; Nina Papavasiliou and Danae Schulz for useful comments; Lars Dölken, Noélia Custódio and Célia Carvalho for the helpful recommendations on the 4sU experiments. This work was supported in part by FCG (P-105333), FCT (PTDC/BIA-BCM/115864/2009), Marie Curie Reintegration Grant (FP7-PEOPLE-RG-2009 'HistoneH1Tryp'), EMBO Installation grant (Project 2151) and Howard Hughes Medical Institute International Early Career Scientist Program (55007419) to L.M.F. and PTDC/BIA-BCM/101575/2008 to M.C.-F. L.P.C. was supported by FCT (grant PTDC/SAU-GMG/115652/2008). A.C.P., F.R.-F., F.A.-B. and R.V.-D. were supported by the fellowships SFRH/BD/73998/2010, SFRH/BD/51286/2010, SFRH/BD/80718/2011 and SFRH/BD/90231/2012 respectively. N.L.B.-M. was supported by a Marie Curie International Outgoing Fellowship (FP7-PEOPLE-2010-IOF 'EvoAltSplice'). The authors declare that they have no conflict of interest.

References

Alibu, V.P., Storm, L., Haile, S., Clayton, C., and Horn, D. (2005) A doubly inducible system for RNA interference and rapid RNAi plasmid construction in *Trypanosoma brucei*. *Mol Biochem Parasitol* **139:** 75–82.

Allan, J., Hartman, P.G., Crane-Robinson, C., and Aviles, F.X. (1980) The structure of histone H1 and its location in chromatin. *Nature* **288:** 675–679.

Alsford, S., Kawahara, T., Glover, L., and Horn, D. (2005) Tagging a *T. brucei* RRNA locus improves stable transfection efficiency and circumvents inducible expression position effects. *Mol Biochem Parasitol* **144:** 142–148.

Anders, S., and Huber, W. (2010) Differential expression analysis for sequence count data. *Genome Biol* **11:** R106.

Bednar, J., Horowitz, R.A., Grigoryev, S.A., Carruthers, L.M., Hansen, J.C., Koster, A.J., and Woodcock, C.L. (1998) Nucleosomes, linker DNA, and linker histone form a unique structural motif that directs the higher-order folding and compaction of chromatin. *Proc Natl Acad Sci USA* **95:** 14173–14178.

Benjamini, Y., and Hochberg, Y. (1995) Controlling the false discovery rate – a practical and powerful approach to multiple testing. *J Roy Stat Soc B* **57:** 289–300.

Berriman, M., Ghedin, E., Hertz-Fowler, C., Blandin, G., Renauld, H., Bartholomeu, D.C., *et al*. (2005) The genome of the African trypanosome *Trypanosoma brucei*. *Science* **309:** 416–422.

Burri, M., Schlimme, W., Betschart, B., and Hecker, H. (1994) Characterization of the histones of *Trypanosoma brucei brucei* bloodstream forms. *Acta Trop* **58:** 291–305.

Burri, M., Schlimme, W., Betschart, B., Lindner, H., Kampfer, U., Schaller, J., and Hecker, H. (1995) Partial amino acid sequence and functional aspects of histone H1 proteins in *Trypanosoma brucei brucei*. *Biol Cell* **83:** 23–31.

Clayton, C., and Shapira, M. (2007) Post-transcriptional regulation of gene expression in trypanosomes and leishmanias. *Mol Biochem Parasitol* **156:** 93–101.

Cock, P.J., Fields, C.J., Goto, N., Heuer, M.L., and Rice, P.M. (2010) The Sanger FASTQ file format for sequences with quality scores, and the Solexa/Illumina FASTQ variants. *Nucleic Acids Res* **38:** 1767–1771.

Dacks, J.B., Walker, G., and Field, M.C. (2008) Implications of the new eukaryotic systematics for parasitologists. *Parasitol Int* **57:** 97–104.

Denninger, V., Fullbrook, A., Bessat, M., Ersfeld, K., and Rudenko, G. (2010) The FACT subunit TbSpt16 is involved in cell cycle specific control of VSG expression sites in *Trypanosoma brucei*. *Mol Microbiol* **78:** 459–474.

Dolken, L., Ruzsics, Z., Radle, B., Friedel, C.C., Zimmer, R., Mages, J., *et al*. (2008) High-resolution gene expression profiling for simultaneous kinetic parameter analysis of RNA synthesis and decay. *RNA* **14:** 1959–1972.

Donelson, J.E. (2003) Antigenic variation and the African trypanosome genome. *Acta Trop* **85:** 391–404.

Downs, J.A., Kosmidou, E., Morgan, A., and Jackson, S.P. (2003) Suppression of homologous recombination by the *Saccharomyces cerevisiae* linker histone. *Mol Cell* **11:** 1685–1692.

Fan, Y., Nikitina, T., Morin-Kensicki, E.M., Zhao, J., Magnuson, T.R., Woodcock, C.L., and Skoultchi, A.I. (2003) H1 linker histones are essential for mouse development and affect nucleosome spacing *in vivo*. *Mol Cell Biol* **23:** 4559–4572.

Fan, Y., Nikitina, T., Zhao, J., Fleury, T.J., Bhattacharyya, R., Bouhassira, E.E., *et al*. (2005) Histone H1 depletion in mammals alters global chromatin structure but causes specific changes in gene regulation. *Cell* **123:** 1199–1212.

Figueiredo, L.M., and Cross, G.A. (2010) Nucleosomes are depleted at the VSG expression site transcribed by RNA polymerase I in African trypanosomes. *Eukaryot Cell* **9:** 148–154.

Giresi, P.G., Kim, J., McDaniell, R.M., Iyer, V.R., and Lieb, J.D. (2007) FAIRE (Formaldehyde-Assisted Isolation of Regulatory Elements) isolates active regulatory elements from human chromatin. *Genome Res* **17:** 877–885.

Grüter, E., and Betschart, B. (2001) Isolation, characterisation and organisation of histone H1 genes in African trypanosomes. *Parasitol Res* **87:** 977–984.

Gunzl, A., Bruderer, T., Laufer, G., Schimanski, B., Tu, L.C., Chung, H.M., *et al*. (2003) RNA polymerase I transcribes procyclin genes and variant surface glycoprotein gene expression sites in *Trypanosoma brucei*. *Eukaryot Cell* **2:** 542–551.

Haenni, S., Renggli, C.K., Fragoso, C.M., Oberle, M., and Roditi, I. (2006) The procyclin-associated genes of *Trypanosoma brucei* are not essential for cyclical transmission by tsetse. *Mol Biochem Parasitol* **150:** 144–156.

Hashimoto, H., Takami, Y., Sonoda, E., Iwasaki, T., Iwano, H., Tachibana, M., *et al*. (2010) Histone H1 null vertebrate cells exhibit altered nucleosome architecture. *Nucleic Acids Res* **38:** 3533–3545.

Hellauer, K., Sirard, E., and Turcotte, B. (2001) Decreased expression of specific genes in yeast cells lacking histone H1. *J Biol Chem* **276:** 13587–13592.

Hertz-Fowler, C., Figueiredo, L.M., Quail, M.A., Becker, M.,

Jackson, A., Bason, N., *et al*. (2008) Telomeric expression sites are highly conserved in *Trypanosoma brucei*. *PLoS ONE* **3:** e3527.

Hill, D.A., and Reeves, R. (1997) Competition between HMG-I(Y), HMG-1 and histone H1 on four-way junction DNA. *Nucleic Acids Res* **25:** 3523–3531.

Hirumi, H., and Hirumi, K. (1989) Continuous cultivation of *Trypanosoma brucei* blood stream forms in a medium containing a low concentration of serum protein without feeder cell layers. *J Parasitol* **75:** 985–989.

Hughes, K., Wand, M., Foulston, L., Young, R., Harley, K., Terry, S., *et al*. (2007) A novel ISWI is involved in VSG expression site downregulation in African trypanosomes. *EMBO J* **26:** 2400–2410.

Izzo, A., Kamieniarz, K., and Schneider, R. (2008) The histone H1 family: specific members, specific functions? *Biol Chem* **389:** 333–343.

Johnson, J.G., and Cross, G.A. (1979) Selective cleavage of variant surface glycoproteins from *Trypanosoma brucei*. *Biochem J* **178:** 689–697.

Kasinsky, H.E., Lewis, J.D., Dacks, J.B., and Ausio, J. (2001) Origin of H1 linker histones. *FASEB J* **15:** 34–42.

Kim, H.S., Park, S.H., Gunzl, A., and Cross, G.A. (2013) MCM-BP is required for repression of life-cycle specific genes transcribed by RNA polymerase I in the mammalian infectious form of *Trypanosoma brucei*. *PLoS ONE* **8:** e57001.

Langmead, B., Trapnell, C., Pop, M., and Salzberg, S.L. (2009) Ultrafast and memory-efficient alignment of short DNA sequences to the human genome. *Genome Biol* **10:** R25.

Laybourn, P.J., and Kadonaga, J.T. (1991) Role of nucleosomal cores and histone H1 in regulation of transcription by RNA polymerase II. *Science* **254:** 238–245.

Lecordier, L., Walgraffe, D., Devaux, S., Poelvoorde, P., Pays, E., and Vanhamme, L. (2005) *Trypanosoma brucei* RNA interference in the mammalian host. *Mol Biochem Parasitol* **140:** 127–131.

Luger, K., Mader, A.W., Richmond, R.K., Sargent, D.F., and Richmond, T.J. (1997) Crystal structure of the nucleosome core particle at 2.8 A resolution. *Nature* **389:** 251–260.

Lundin, C., North, M., Erixon, K., Walters, K., Jenssen, D., Goldman, A.S., and Helleday, T. (2005) Methyl methanesulfonate (MMS) produces heat-labile DNA damage but no detectable *in vivo* DNA double-strand breaks. *Nucleic Acids Res* **33:** 3799–3811.

Marcello, L., and Barry, J.D. (2007) Analysis of the VSG gene silent archive in *Trypanosoma brucei* reveals that mosaic gene expression is prominent in antigenic variation and is favored by archive substructure. *Genome Res* **17:** 1344–1352.

Masina, S., Zangger, H., Rivier, D., and Fasel, N. (2007) Histone H1 regulates chromatin condensation in *Leishmania* parasites. *Exp Parasitol* **116:** 83–87.

Murga, M., Jaco, I., Fan, Y., Soria, R., Martinez-Pastor, B., Cuadrado, M., *et al*. (2007) Global chromatin compaction limits the strength of the DNA damage response. *J Cell Biol* **178:** 1101–1108.

Narayanan, M.S., Kushwaha, M., Ersfeld, K., Fullbrook, A., Stanne, T.M., and Rudenko, G. (2011) NLP is a novel transcription regulator involved in VSG expression site control in *Trypanosoma brucei*. *Nucleic Acids Res* **39:** 2018–2031.

Navarro, M., Penate, X., and Landeira, D. (2007) Nuclear architecture underlying gene expression in *Trypanosoma brucei*. *Trends Microbiol* **15:** 263–270.

Nguyen, T.N., Muller, L.S., Park, S.H., Siegel, T.N., and Gunzl, A. (2014) Promoter occupancy of the basal class I transcription factor A differs strongly between active and silent VSG expression sites in *Trypanosoma brucei*. *Nucleic Acids Res* **42:** 3164–3176.

Nilsson, D., Gunasekera, K., Mani, J., Osteras, M., Farinelli, L., Baerlocher, L., *et al*. (2010) Spliced leader trapping reveals widespread alternative splicing patterns in the highly dynamic transcriptome of *Trypanosoma brucei*. *PLoS Pathog* **6:** e1001037.

Noble, W.S. (2009) How does multiple testing correction work? *Nat Biotechnol* **27:** 1135–1137.

Noll, M., and Kornberg, R.D. (1977) Action of micrococcal nuclease on chromatin and the location of histone H1. *J Mol Biol* **109:** 393–404.

Patterton, H.G., Landel, C.C., Landsman, D., Peterson, C.L., and Simpson, R.T. (1998) The biochemical and phenotypic characterization of Hho1p, the putative linker histone H1 of *Saccharomyces cerevisiae*. *J Biol Chem* **273:** 7268–7276.

Pays, E., Vanhamme, L., and Perez-Morga, D. (2004) Antigenic variation in *Trypanosoma brucei*: facts, challenges and mysteries. *Curr Opin Microbiol* **7:** 369–374.

Pfaffl, M.W. (2001) A new mathematical model for relative quantification in real-time RT-PCR. *Nucleic Acids Res* **29:** e45.

Povelones, M.L., Gluenz, E., Dembek, M., Gull, K., and Rudenko, G. (2012) Histone H1 plays a role in heterochromatin formation and VSG expression site silencing in *Trypanosoma brucei*. *PLoS Pathog* **8:** e1003010.

Rabani, M., Levin, J.Z., Fan, L., Adiconis, X., Raychowdhury, R., Garber, M., *et al*. (2011) Metabolic labeling of RNA uncovers principles of RNA production and degradation dynamics in mammalian cells. *Nat Biotechnol* **29:** 436–442.

Robinson, P.J., and Rhodes, D. (2006) Structure of the '30 nm' chromatin fibre: a key role for the linker histone. *Curr Opin Struct Biol* **16:** 336–343.

Rudenko, G., Bishop, D., Gottesdiener, K., and Van der Ploeg, L.H. (1989) Alpha-amanitin resistant transcription of protein coding genes in insect and bloodstream form *Trypanosoma brucei*. *EMBO J* **8:** 4259–4263.

Sanicola, M., Ward, S., Childs, G., and Emmons, S.W. (1990) Identification of a *Caenorhabditis elegans* histone H1 gene family. Characterization of a family member containing an intron and encoding a poly(A) + mRNA. *J Mol Biol* **212:** 259–268.

Shen, X., and Gorovsky, M.A. (1996) Linker histone H1 regulates specific gene expression but not global transcription *in vivo*. *Cell* **86:** 475–483.

Shen, X., Yu, L., Weir, J.W., and Gorovsky, M.A. (1995) Linker histones are not essential and affect chromatin condensation *in vivo*. *Cell* **82:** 47–56.

Shimamura, A., Sapp, M., Rodriguez-Campos, A., and Worcel, A. (1989) Histone H1 represses transcription from minichromosomes assembled *in vitro*. *Mol Cell Biol* **9:** 5573–5584.

Siegel, T.N., Hekstra, D.R., Kemp, L.E., Figueiredo, L.M., Lowell, J.E., Fenyo, D., *et al*. (2009) Four histone variants mark the boundaries of polycistronic transcription units in *Trypanosoma brucei*. *Genes Dev* **23:** 1063–1076.

Simpson, A.G., and Roger, A.J. (2004) The real 'kingdoms' of eukaryotes. *Curr Biol* **14:** R693–R696.

Smirlis, D., Bisti, S.N., Xingi, E., Konidou, G., Thiakaki, M., and Soteriadou, K.P. (2006) Leishmania histone H1 overexpression delays parasite cell-cycle progression, parasite differentiation and reduces *Leishmania* infectivity *in vivo*. *Mol Microbiol* **60:** 1457–1473.

Stanne, T.M., and Rudenko, G. (2010) Active VSG expression sites in *Trypanosoma brucei* are depleted of nucleosomes. *Eukaryot Cell* **9:** 136–147.

Subramanian, A., Tamayo, P., Mootha, V.K., Mukherjee, S., Ebert, B.L., Gillette, M.A., *et al*. (2005) Gene set enrichment analysis: a knowledge-based approach for interpreting genome-wide expression profiles. *Proc Natl Acad Sci USA* **102:** 15545–15550.

Talbert, P.B., Ahmad, K., Almouzni, G., Ausio, J., Berger, F., Bhalla, P.L., *et al*. (2012) A unified phylogeny-based nomenclature for histone variants. *Epigenetics Chromatin* **5:** 7.

Thoma, F., Koller, T., and Klug, A. (1979) Involvement of histone H1 in the organization of the nucleosome and of the salt-dependent superstructures of chromatin. *J Cell Biol* **83:** 403–427.

Vanhamme, L., Poelvoorde, P., Pays, A., Tebabi, P., Van Xong, H., and Pays, E. (2000) Differential RNA elongation controls the variant surface glycoprotein gene expression sites of *Trypanosoma brucei*. *Mol Microbiol* **36:** 328–340.

Vujatovic, O., Zaragoza, K., Vaquero, A., Reina, O., Bernues, J., and Azorin, F. (2012) Drosophila melanogaster linker histone dH1 is required for transposon silencing and to preserve genome integrity. *Nucleic Acids Res* **40:** 5402–5414.

Wang, Q.P., Kawahara, T., and Horn, D. (2010) Histone deacetylases play distinct roles in telomeric VSG expression site silencing in African trypanosomes. *Mol Microbiol* **77:** 1237–1245.

Windhager, L., Bonfert, T., Burger, K., Ruzsics, Z., Krebs, S., Kaufmann, S., *et al*. (2012) Ultrashort and progressive 4sU-tagging reveals key characteristics of RNA processing at nucleotide resolution. *Genome Res* **22:** 2031–2042.

Yang, X., Figueiredo, L.M., Espinal, A., Okubo, E., and Li, B. (2009) RAP1 is essential for silencing telomeric variant surface glycoprotein genes in *Trypanosoma brucei*. *Cell* **137:** 99–109.

Supporting information

Additional supporting information may be found in the online version of this article at the publisher's web-site.